

Alma Mater Studiorum Università di Bologna  
Archivio istituzionale della ricerca

Assessing the effects of covalent, dative and halogen bonds on the electronic structure of selenoamides

This is the final peer-reviewed author's accepted manuscript (postprint) of the following publication:

*Published Version:*

Ciancaleoni, G., Marchetti, F., Santi, C., Merlino, O., Zacchini, S. (2022). Assessing the effects of covalent, dative and halogen bonds on the electronic structure of selenoamides. NEW JOURNAL OF CHEMISTRY, 46, 10568-10576 [10.1039/d2nj01421a].

*Availability:*

This version is available at: <https://hdl.handle.net/11585/897662> since: 2023-06-09

*Published:*

DOI: <http://doi.org/10.1039/d2nj01421a>

*Terms of use:*

Some rights reserved. The terms and conditions for the reuse of this version of the manuscript are specified in the publishing policy. For all terms of use and more information see the publisher's website.

This item was downloaded from IRIS Università di Bologna (<https://cris.unibo.it/>).  
When citing, please refer to the published version.

(Article begins on next page)

This is the final peer-reviewed accepted manuscript of:

G. Ciancaleoni, F. Marchetti, C. Santi, O. Merlino, S. Zacchini, "Assessing the effects of covalent, dative and halogen bond on the electronic structure of selenoamides", *New. J. Chem.*, **2022**, 46, 10568-10576.

The final published version is available online at:

[https://doi.org/ 10.1039/d2nj01421a](https://doi.org/10.1039/d2nj01421a)

#### Terms of use:

Some rights reserved. The terms and conditions for the reuse of this version of the manuscript are specified in the publishing policy. For all terms of use and more information see the publisher's website.

This item was downloaded from IRIS Università di Bologna (<https://cris.unibo.it/>)

**When citing, please refer to the published version.**

# Assessing the effects of covalent, dative and halogen bond on the electronic structure of selenoamide

Gianluca Ciancaleoni,\*<sup>[a]</sup>Fabio Marchetti,<sup>[a]</sup> Claudio Santi,<sup>[b]</sup> Orsola Merlino,<sup>[b]</sup> Stefano Zacchini<sup>[c]</sup>

<sup>[a]</sup> Prof. Dr. G. Ciancaleoni, Prof. Dr. F. Marchetti

Dipartimento di Chimica e Chimica Industriale, Università degli studi di Pisa, via Giuseppe Moruzzi 13, 56124, Italy

E-mail: gianluca.ciancaleoni@unipi.it

<sup>[b]</sup> Prof. Dr. C. Santi, O. Merlino

Dipartimento di Scienze Farmaceutiche, Università degli studi di Perugia, via del Liceo, 06132, Perugia, Italy

<sup>[c]</sup> Prof. Dr. S. Zacchini

Dipartimento di Chimica Fisica ed Inorganica, Università di Bologna, viale Risorgimento 4, 40136 Bologna, Italy

## ABSTRACT

The interaction between N,N-dimethyl-selenobenzoamide  $\text{PhC(=Se)NMe}_2$  (**1**) and various Lewis acids of different strength, namely  $\text{IC}_6\text{F}_{13}$  (**I**),  $\text{B(C}_6\text{F}_5)_3$  (**B**) and  $\text{Me}^+$ , has been analysed here by a combined experimental and theoretical approach. In all the cases, an increase of the C-NMe<sub>2</sub> rotational barrier has been evidenced and quantified by <sup>1</sup>H-Variable Temperature-Exchange NMR Spectroscopy (VT-EXSY) in the cases of **1-I** and **1-B**. For  $\text{B(C}_6\text{F}_5)_3$ , the structure of the adduct has been elucidated by single crystal X-ray diffraction, allowing to measure the lengthening of Se-B bond (216.7 pm) and the consequent double character of the C-NMe<sub>2</sub> bond. Computational studies (mainly Natural Bond Orbitals and Natural Orbital for Chemical Valence analyses) give precious insight to the effect of the various Lewis acids on the electronic structure of **1**. The advantage and the limitations of this new method to characterize chemical interactions is discussed.

## 1. INTRODUCTION

This item was downloaded from IRIS Università di Bologna (<https://cris.unibo.it/>)

**When citing, please refer to the published version.**

The nature of halogen bond (XB<sup>[1,2]</sup>) is still a matter of debate, in particular about the importance of the different bond contributions, as electrostatics, covalency and dispersion.<sup>[3,4]</sup> In the past, the general idea was that XB and covalent bonds are ontologically different and refer to different phenomena. But it is now accepted that a non-negligible amount of orbital contribution is present in the XB,<sup>[5]</sup> the importance of which depends on the nature (polarizability, charge) of the interacting moieties. This new piece of information thinned the differences between covalent and “non-covalent” interactions, making them more similar from the philosophical point of view. In fact, the idea underlying the Energy Decomposition Analysis (EDA)<sup>[6,7]</sup> and other similar decomposition schemes is that all the chemical interactions can be characterized by a few physically meaningful descriptors. In the canonical EDA, they are electrostatics, orbital interaction and Pauli repulsion (with dispersion if the functional supports it).

It has to be said that most of the bond analysis is theoretical,<sup>[8]</sup> since finding a non-ambiguous experimental observable is not straightforward. When the tendency to co-crystallize is strong enough, the distance between XB donors and acceptors can be directly measured and compared,<sup>[9]</sup> revealing that there could not be a clear-cut separation between covalent and non-covalent bonds, but such studies are not always possible.

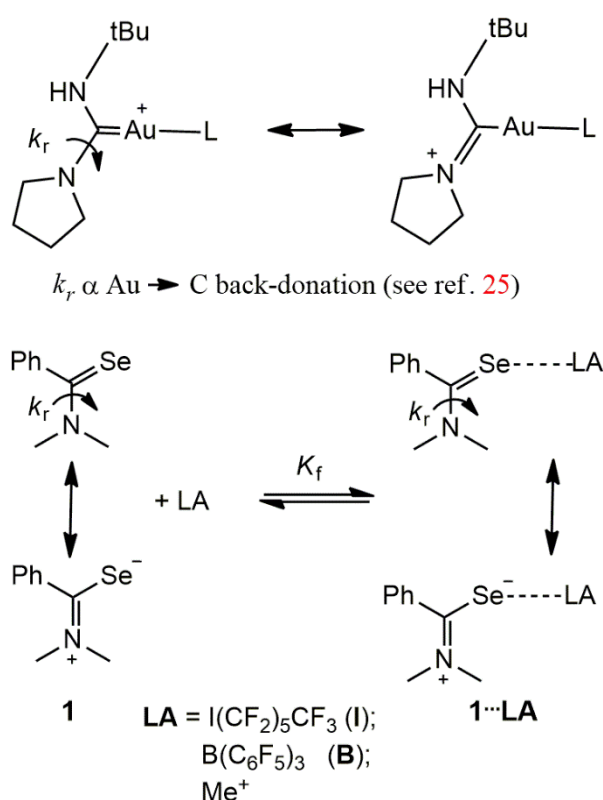
Even more challenging is the solution world,<sup>[10,11]</sup> where internuclear distances are not directly accessible. Therefore, other techniques whose output depends on the presence of the interaction are employed: some examples are UV-VIS spectroscopy,<sup>[12]</sup> IR-Raman spectroscopies<sup>[13]</sup> and NMR spectroscopy, either with monodimensional<sup>[14–17]</sup> and advanced techniques.<sup>[18–22]</sup>

Recently, the rotation of a chemical bond monitored by exchange spectroscopy (EXSY) NMR has been successfully applied in the quest for an experimental probe of back-donation in metal complexes.<sup>[23–25]</sup> As the results have been very promising for the characterization of the metal-ligand coordinative bond, we took advantage of the same idea and we designed a system that is able to establish many kinds of bonds, either covalent and not, with the ambitious idea to use its experimental properties to characterize the interaction.

We found a suitable candidate in the selenoamide **1** depicted in Scheme 1. The lone pairs of the selenium can establish various chemical interactions: halogen bond with IC<sub>6</sub>F<sub>13</sub>,<sup>[26]</sup> dative bond with the electron-deficient B(C<sub>6</sub>F<sub>5</sub>)<sub>3</sub><sup>[27,28]</sup> or covalent bond with the methyl group.<sup>[29]</sup> On the other hand, the nature of the C-N bond depends on the C-Se bond, as the two are connected by resonance

(Scheme 1). Therefore, the rotation rate of the C-N bond can be, in principle, measured by EXSY NMR and it will be proportional to the bond order of the C-Se bond.

Scheme 1 compares the gold system used in literature<sup>[25]</sup> and **1**. For the former, the nitrogen acyclic carbene (NAC) ligand was a good probe of the Au  $\rightarrow$  C back-donation, which in its turn was modulated by the second ligand L, spanning from chloride to phenyl to perfluorinated phosphines. Theoretical evaluation of the back-donation correlated linearly with the experimental values of the C-N rotational barrier ( $\Delta H_r^\ddagger$ ).



**Scheme 1.** (Up) Correlation between the L-modulated Au  $\rightarrow$  C back-donation and C-N rotational rate. (Down) Formation and contributing resonance structures of the **1**...LA adduct.  $K_f$  is the formation constant of the adduct and  $k_r$  is the rotational kinetic constant of the C-N bond.

We expect a modulation of  $\Delta H_r^\ddagger$  also in the case of **1** because the C-N bond of selenoamides has been known to be partially double since 1969.<sup>[30]</sup> This implies that also the C-Se bond is partially double and, indeed, its length can be influenced by coordination of C=Se to a metal center<sup>[29,31]</sup> (even if not all the metals have an appreciable effect<sup>[32]</sup>) or a boron trihalide<sup>[33]</sup> and, by weaker

secondary interactions, as hydrogen bonding.<sup>[34]</sup> Therefore, it can be supposed that  $\Delta H_r^\ddagger$  will vary in the presence of different Lewis Acids (LAs). Regarding XB, selenium is nucleophilic enough to establish good XB with adequately polarized halogens,<sup>[35–38]</sup> even if it not routinely used as XB acceptor.

Here, we present the advantages and the limits of our strategy to characterize different interactions involving selenium.

## 2. EXPERIMENTAL

**General Data.** All reactions were routinely carried out under a nitrogen atmosphere, using standard Schlenk techniques. Solvents (except deuterated ones) were distilled immediately before use under nitrogen from the appropriate drying agents. All the reagents were commercial products of the highest purity available and were used as received. **1** was synthesized following the literature procedure.<sup>[39]</sup> NMR spectra were recorded on a Bruker Avance II DRX400 instrument equipped with a BBFO broadband probe. Chemical shifts (expressed in parts permillion) are referenced to the residual solvent peaks (<sup>1</sup>H, <sup>13</sup>C) or to external standards. Carbon, hydrogen and nitrogen analyses were performed on a Vario MICRO cube instrument (Elementar).

### Synthesis and characterization of **1-B**.

A suspension of **1** (50 mg, 0.236 mmol) and B(C<sub>6</sub>F<sub>5</sub>)<sub>3</sub> (120 mg, 0.236 mmol) in dry *n*-pentane was stirred for 1 h. The solid went from orange to white and was filtered and redissolved in dry CH<sub>2</sub>Cl<sub>2</sub>, giving an orange solution. Crystals suitable for X-ray analysis were obtained by a CH<sub>2</sub>Cl<sub>2</sub> solution layered with pentane. Anal. Calcd for C<sub>27</sub>H<sub>11</sub>BF<sub>15</sub>N<sub>2</sub>Se: C, 43.92; H, 1.50; N, 3.80. Found: C, 43.82; H, 1.74; N, 3.54.

<sup>1</sup>H NMR (400 MHz, C<sub>6</sub>D<sub>6</sub>, 300 K,  $\delta$  in ppm, *J* in Hz): 6.88 (t, <sup>3</sup>*J*<sub>HH</sub> = 7.5, 1H, *p*-H), 6.71 (t, <sup>3</sup>*J*<sub>HH</sub> = 7.7, 2H, *m*-H), 6.45 (d, <sup>3</sup>*J*<sub>HH</sub> = 7.6, 2H, *o*-H), 2.45 (s, 3H, Me<sup>B</sup>), 1.54 (s, 3H, Me<sup>A</sup>). <sup>13</sup>C{<sup>1</sup>H} NMR (100 MHz, C<sub>6</sub>D<sub>6</sub>, 300 K,  $\delta$  in ppm, *J* in Hz): 200.62 (s, C=Se), 148.13 (dm, <sup>1</sup>*J*<sub>CF</sub> = 242, *o*-C of C<sub>6</sub>F<sub>5</sub>), 139.91 (dm, <sup>1</sup>*J*<sub>CF</sub> = 250, *p*-C of C<sub>6</sub>F<sub>5</sub>), 137.13 (dm, <sup>1</sup>*J*<sub>CF</sub> = 246, *m*-C of C<sub>6</sub>F<sub>5</sub>), 136.44 (s, *ipso*-C of C<sub>6</sub>H<sub>5</sub>), 130.40 (s, *p*-C of C<sub>6</sub>H<sub>5</sub>), 128.37 (s, *m*-C of C<sub>6</sub>H<sub>5</sub>), 124.57 (s, *o*-C of C<sub>6</sub>H<sub>5</sub>), 118.82 (m, *ipso*-C of C<sub>6</sub>F<sub>5</sub>), 45.82 (s, Me<sup>B</sup>), 44.30 (s, Me<sup>A</sup>). <sup>19</sup>F NMR (377 MHz, C<sub>6</sub>D<sub>6</sub>, 300 K,  $\delta$  in ppm, *J* in Hz): -129.74 (br d, <sup>3</sup>*J*<sub>FF</sub> = 19.0, *o*-F), -157.84 (br t, <sup>3</sup>*J*<sub>FF</sub> = 20.7, *p*-F), -164.61 (br t, <sup>3</sup>*J*<sub>FF</sub> = 19.1, *m*-F). <sup>77</sup>Se

NMR (s, 76.54 MHz C<sub>6</sub>D<sub>6</sub>, 300 K,  $\delta$  in ppm): 578.5. <sup>11</sup>B NMR (128.77 MHz, C<sub>6</sub>D<sub>6</sub>, 300 K,  $\delta$  in ppm): -6.22 (br). IR (KBr) 1532 cm<sup>-1</sup> (C=Se).

### Synthesis and characterization of 1-Me<sup>+</sup>I<sup>-</sup>.

In a NMR tube, **1** (4.4 mg) was added to a 1 mL solution of MeI in C<sub>6</sub>D<sub>6</sub> (48 mM), in order to have a final concentration of **1** = 21 mM. The reaction was conducted either in the presence or absence of IC<sub>6</sub>F<sub>13</sub> (0.8 M). The tube was vigorously shaken for 30 seconds and inserted in the NMR spectrometer to follow the kinetics of formation. The final product was been isolated but NMR spectroscopic information are in agreement with those reported in literature,<sup>[29]</sup> with small differences due to the solvent and counterion (CDCl<sub>3</sub> and triflate in the reported paper, C<sub>6</sub>D<sub>6</sub> and iodide here).

<sup>1</sup>H NMR (400 MHz, C<sub>6</sub>D<sub>6</sub>, 300 K,  $\delta$  in ppm, *J* in Hz): <sup>13</sup>C{<sup>1</sup>H} NMR (100 MHz C<sub>6</sub>D<sub>6</sub>, 300 K,  $\delta$  in ppm): 195.85 (s, C=Se), 132.33 (s, *p*-C of C<sub>6</sub>H<sub>5</sub>), 131.83 (s, *ipso*-C of C<sub>6</sub>H<sub>5</sub>), 130.05 (s, *m*-C of C<sub>6</sub>H<sub>5</sub>), 126.55 (s, *o*-C of C<sub>6</sub>H<sub>5</sub>), 49.88 (s, Me<sup>A</sup>), 48.62 (s, Me<sup>B</sup>), 13.83 (s, Se-CH<sub>3</sub>). <sup>77</sup>Se NMR (s, 76.54 MHz C<sub>6</sub>D<sub>6</sub>, 300 K,  $\delta$  in ppm): 459.0.

### X-ray crystallography.

Crystal data and collection details for **1-B** are reported in Table 1. Data were recorded on a Bruker APEX II diffractometer equipped with a PHOTON100 detector using Mo-K $\alpha$  radiation. Data were corrected for Lorentz polarization and absorption effects (empirical absorption correction SADABS).<sup>[40]</sup> The structure was solved by direct methods and refined by full-matrix least-squares based on all data using F2.<sup>[41]</sup> Hydrogen atoms were fixed at calculated positions and refined by a riding model. All non-hydrogen atoms were refined with anisotropic displacement parameters. The crystals appeared to be non-merohedrally twinned. The TwinRotMat routine of PLATON<sup>[42]</sup> was used to determine the twinning matrix and to write the reflection data file (.hkl) containing the two twin components. Refinement was performed using the instruction HKLF 5 in SHELXL and one BASF parameter, which refined as 0.2952(10). Two independent molecules possessing very similar geometries and bonding parameters were present within the unit cell.

**Table 1.** Crystal data and measurement details for **1-B**.

**1-B**

This item was downloaded from IRIS Università di Bologna (<https://cris.unibo.it/>)

**When citing, please refer to the published version.**

Formula	C <sub>27</sub> H <sub>11</sub> BF <sub>15</sub> NSe
FW	724.14
T, K	100(2)
$\lambda$ , Å	0.71073
Crystal system	Triclinic
Space group	$P\bar{1}$
$a$ , Å	12.9884(9)
$b$ , Å	14.0613(10)
$c$ , Å	16.1245(12)
$\alpha$ , °	69.146(2)
$\beta$ , °	70.272(2)
$\gamma$ , °	76.363(3)
Cell Volume, Å <sup>3</sup>	2568.1(3)
Z	4
$D_c$ , g·cm <sup>-3</sup>	1.873
$\mu$ , mm <sup>-1</sup>	1.593
F(000)	1416
Crystal size, mm	0.25 × 0.20 × 0.15
$\theta$ limits, °	1.563 - 26.000
Reflections collected	33693
Independent reflections	10045 [ $R_{int} = 0.0684$ ]
Data / restraints / parameters	10045 / 0 / 812
Goodness on fit on F <sup>2</sup>	1.029
$R_1$ ( $I > 2\sigma(I)$ )	0.0493
$wR_2$ (all data)	0.1118
Largest diff. peak and hole, e Å <sup>-3</sup>	0.694 / -0.636

## PGSE NMR.

<sup>1</sup>H PGSE NMR measurements were performed by using the double-stimulated echo sequence with longitudinal eddy current delay<sup>[43]</sup> at 298 K without spinning. The dependence of the resonance intensity ( $I$ ) on a constant waiting time and on a varied gradient strength  $G$  is described by the following equation (1):

$$\ln \frac{I}{I_0} = (\gamma\delta)^2 D_t \left( \Delta - \frac{\delta}{3} \right) G^2 (1)$$

where  $I$  is the intensity of the observed spin echo,  $I_0$  the intensity of the spin echo in the absence of gradient,  $D_t$  the self-diffusion coefficient,  $\Delta$  the delay between the midpoints of the gradients (0.2 s),  $\delta$  the length of the gradient pulse (4 ms), and  $\gamma$  the magnetogyric ratio. The shape of the gradients was rectangular, their length  $\delta$  was 4–5 ms, and their strength  $G$  was varied during the experiments.

This item was downloaded from IRIS Università di Bologna (<https://cris.unibo.it/>)

**When citing, please refer to the published version.**



The self-diffusion coefficient  $D_t$ , was estimated by evaluating the proportionality constant for a sample of HDO (5%) in  $D_2O$  [known diffusion coefficients in the range 274–318 K<sup>[44]</sup>] under the exact same conditions as the sample of interest. The solvent or TMS was taken as internal standard. Since the aromatic protons of **S** overlap with the residual solvent peak of  $C_6D_6$ , the latter cannot be used as internal reference, as usually done.<sup>[45]</sup> For this reason, the hydrodynamic properties of dichloromethane in  $C_6D_6$  were determined, in order to use  $CH_2Cl_2$  as internal standard for all the other measurements.

## Computational Details

**Geometry Optimization:** All the geometries were optimized by using ORCA 4.1.0,<sup>[46]</sup> at B3LYP level within RIJK approach in the gas phase. Def2-TZVPD and the corresponding auxiliary basis sets def2/J were used. Dispersion effects were considered using the popular Grimme's correction D3 with BJ damping.<sup>[47,48]</sup> All the optimized geometries showed only positive frequencies, except in the case of **1-BCl<sub>3</sub>**, which showed a small, non-avoidable imaginary frequency not related to the Se-B interaction but associated to a phenyl libration.

NBO analyses were conducted by using NBO7<sup>[49]</sup> in conjunction with ORCA 4.1.0 or, for the NEDA calculations, with Gaussian16. Details about Natural Energy Decomposition Analysis (NEDA)<sup>[50]</sup> and Extended Transition State-Natural Orbital for Chemical Valence (ETS-NOCV)<sup>[51]</sup> are given in the Electronic Supporting Information (ESI).

## 3. RESULTS AND DISCUSSION

**3.1 Experimental studies.** Firstly, we tested the selenoamide properties as XB acceptor, following the  $^{19}F$  chemical shift of the  $-CF_2I$  moiety of **I** in  $C_6D_6$  as the concentration of **1** increases. At 297 K, the formation constant ( $K_f$ ) of the XB adduct resulted to be  $2.59 \pm 0.03 \text{ M}^{-1}$ . Diffusional NMR measurements on a solution 3.2 mM of **1** and 247 mM of **I** gave a very similar value ( $K_f = 2.4 \pm 0.3 \text{ M}^{-1}$ ), with a hydrodynamic volume ( $310 \text{ \AA}^3$ ) that is lower than the sum of the hydrodynamic volumes of **1** and **I** ( $230$  and  $220 \text{ \AA}^3$ , respectively). The large excess of **I** served to favor the formation of higher adducts (as  $1:2^{[35]}$ ), if possible, but under our conditions they can be ruled out. Titrations have been conducted also at higher temperatures and, at the highest T value studied (325 K),  $K_f$  decreased to  $1.65 \pm 0.03 \text{ M}^{-1}$  (Table 1). From these measurements, it is possible to estimate

*This item was downloaded from IRIS Università di Bologna (<https://cris.unibo.it/>)*

***When citing, please refer to the published version.***

the formation enthalpy at 298 K ( $\Delta H_f$ ) and entropy ( $\Delta S_f$ ) as -3.0 kcal/mol and -8.3 cal/(mol K), respectively.

The rotational barrier of the C-N bond ( $\Delta H_r^\ddagger$ ) was measured by using the Variable Temperature EXSY NMR (Figure 1). The rotational rate constant around the C-N bond ( $k_r$ ) resulted to be  $0.141 \pm 0.005 \text{ s}^{-1}$  at 298 K and it increases up to  $2.30 \pm 0.05 \text{ s}^{-1}$ , as T increases up to 325 K (Table 2).

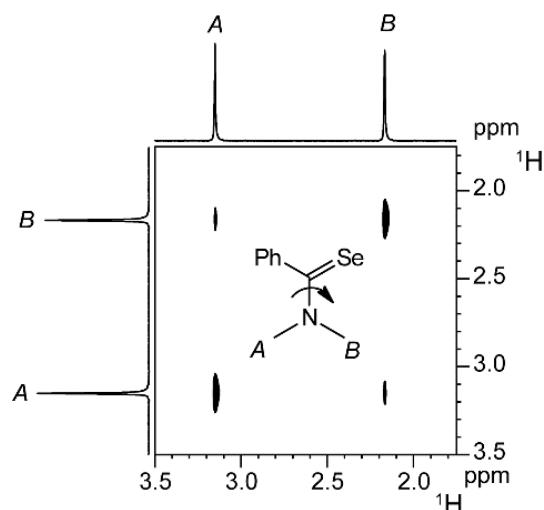


**Figure 1.**  $^1\text{H}$ -EXSY NMR spectrum of **1** (400.13 MHz, 323 K,  $\text{C}_6\text{D}_6$ , mixing time = 150 ms).

**Table 2.** Rotation rates of the  $-\text{NMe}_2$  group ( $k_r$ ), formation constants of the  $\mathbf{1} \cdots \mathbf{I}$  adduct ( $K_f$ ) and  $\mathbf{1} \cdots \mathbf{I}$  concentrations at the different temperatures. In all the cases,  $[\mathbf{1}] = 3.2 \text{ mM}$ .

T (K)	$k_r(\text{s}^{-1})$ ( $[\mathbf{I}] = 0$ )	$k_r(\text{s}^{-1})$ ( $[\mathbf{I}] = 0.8 \text{ M}$ )	$K_f(\text{M}^{-1})$	$[\mathbf{1} \cdots \mathbf{I}] \text{ (mM)}$
298	0.141	n.d. <sup>[a]</sup>	2.59	2.1
303	0.260	0.170	2.36	2.1
309	0.541	0.428	2.15	2.0
317	1.18	0.860	1.94	1.9
325	2.30	2.19	1.65	1.8

[a] Exchange peaks too weak to be integrated

This item was downloaded from IRIS Università di Bologna (<https://cris.unibo.it/>)

**When citing, please refer to the published version.**

Adding a large excess of **I** (0.8 M), enough to guarantee a predominance of the XB adduct (Table 1),  $k_r$  decreases at all the temperature studied.

Fitting the two series of data with the Eyring equation, the values of  $\Delta H_r^\ddagger$  in the absence and in the presence of the Lewis acid can be estimated as  $18.8 \pm 0.3$  and  $21.6 \pm 0.7$  kcal/mol, respectively. The activation entropies are  $0.9 \pm 2$  and  $9 \pm 4$  cal/(mol K), respectively (see ESI). Remarkably, the  $^{77}\text{Se}$  NMR  $\delta$  goes from 802.4 ppm in the absence of **I** to 776.7 ppm in the presence of an excess of **I** (**[I]** and **[I]** 14 and 405 mM, respectively).

All the experimental facts presented here indicate that the formation of the halogen bonding has a measurable effect on the electronic distribution of the selenoamide, increasing the double-bond character of the C-N bond (the rotation becomes more difficult) and the single-bond character of the C-Se bond (the downshift of the NMR  $\delta$  is coherent with a decreasing of the C-Se bond order and the increasing of the zwitterionic resonance structure<sup>[52]</sup>).

The enhanced importance of the zwitterionic resonance structure showed in Scheme 1 can be demonstrated also studying the reactivity of **1** in the presence and in the absence of **I**, respectively. In fact, the reaction between **1** and MeI is accelerated by the presence of an excess of **I** (Figure 2). In both cases, the product has been identified as Se-Methyl-selenouronium iodide ( $[\text{PhC}(-\text{SeMe})\text{NMe}_2]^+ \text{I}^-$ , **1-Me<sup>+</sup>I**)<sup>[29]</sup> which is soluble in benzene only in the presence of **I**, likely because of a XB interaction between the latter and the iodide anion. The acceleration of the reactivity could be due also to a XB between **I** and MeI, which could increase its electrophilicity, but the XB between  $\text{ICF}_3$  (used as a computational model for **I**) and MeI is weaker than that between  $\text{ICF}_3$  and **1** (-4.1 and -10.1 kcal/mol, see ESI). Anyway, being **I** in large excess, it cannot be excluded that both reactants undergo XB.

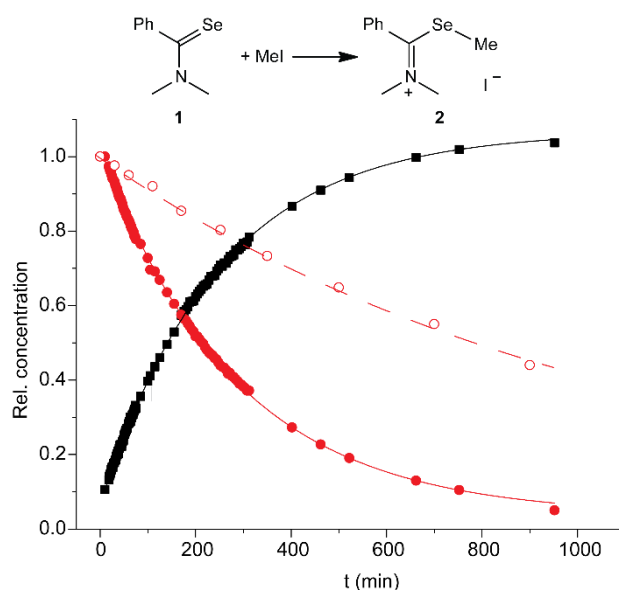


**Figure 2.** Comparison of the reaction rate between **1** (21 mM, red circles) and MeI (48 mM) when  $[I] = 0$  (empty circles) and 0.8 M (full circles). For the latter case, also the growth of the reaction product, **1-Me<sup>+</sup>I** (black squares), is shown.

No rotation of the C-NMe<sub>2</sub> bond could be measured for **1-Me<sup>+</sup>I**, even at the highest temperature allowed by the solvent. This indicates that the C-N bond is essentially double in **1-Me<sup>+</sup>I** and, therefore, the C-Se bond is essentially single.  $\delta_{\text{Se}}(\mathbf{1-Me^+I})$  is 459.0 ppm, in agreement with the reported 449.9 for **1-Me<sup>+</sup>OTf**<sup>[29]</sup> and in the range of diselenide species.<sup>[53]</sup> Indeed, the cation Me<sup>+</sup> can be seen as a very strong Lewis acid that interacts with the selenium and, interestingly, the effect is qualitatively the same than that of **I**, which is an increase of the C-N bond order. Clearly, the extent of this effect is different.

It is now interesting to see the effect of a Lewis acid with intermediate strength between **I** and Me<sup>+</sup> on the structure of **1**, i.e. B(C<sub>6</sub>F<sub>5</sub>)<sub>3</sub> (**B**). To the best of our knowledge, only two examples of Lewis pairs between a C=Se moiety and boron have been characterized,<sup>[27,33]</sup> of which only one at the solid state. Here, we suspended an equimolar amount of **B** and **1** in *n*-pentane, obtaining a solid, which was recrystallized from CH<sub>2</sub>Cl<sub>2</sub>/*n*-pentane.

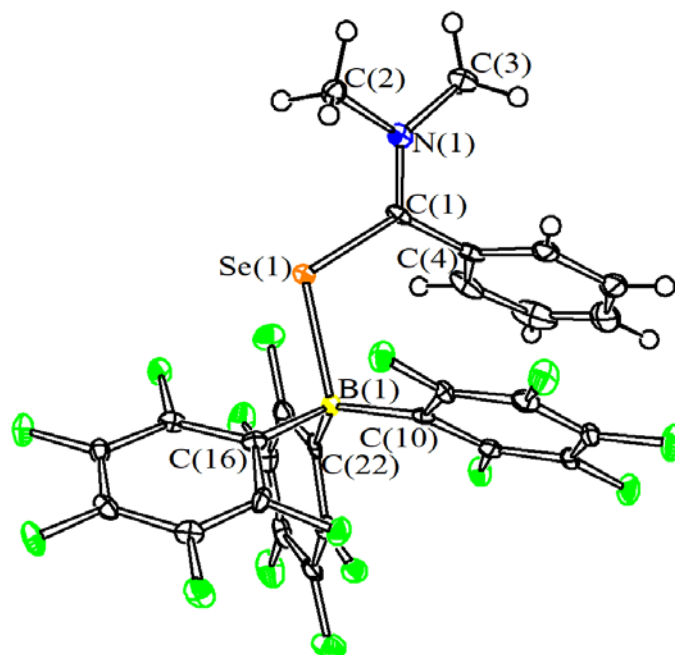


**Figure 3.** Molecular structure of **1-B** with key atoms labelled. Displacement ellipsoids are at the 50% probability level.

The molecular structure of **1-B** is reported in Figure 3 and its most relevant bond distances and angles are summarized in Table 3.

**Table 3.** Selected bond distances (Å) and angles (°) for **1-B** (two independent molecules are present within the unit cell).

	Molecule 1	Molecule 2
N(1)-C(1)	1.310(5)	1.311(5)
N(1)-C(2)	1.460(5)	1.470(5)
N(1)-C(3)	1.477(5)	1.461(5)
C(1)-C(4)	1.473(6)	1.476(6)
C(1)-Se(1)	1.863(4)	1.855(4)
Se(1)-B(1)	2.166(5)	2.168(5)
B(1)-C(10)	1.611(6)	1.629(6)
B(1)-C(16)	1.655(6)	1.658(6)
B(1)-C(22)	1.632(6)	1.624(6)

C(1)-N(1)-C(2)	122.1(4)	124.1(4)
C(1)-N(1)-C(3)	123.5(4)	121.7(3)
C(2)-N(1)-C(3)	114.3(3)	114.0(3)
N(1)-C(1)-C(4)	118.6(4)	119.4(4)
N(1)-C(1)-Se(1)	118.6(3)	117.7(3)
Se(1)-C(1)-C(4)	122.8(3)	122.8(3)
C(1)-Se(1)-B(1)	110.31(18)	112.13(18)
Se(1)-B(1)-C(10)	106.4(3)	107.8(3)
Se(1)-B(1)-C(16)	100.1(3)	97.7(3)
Se(1)-B(1)-C(22)	114.0(3)	113.9(3)

**1-B** consists of a Lewis type acid-base adduct between **1** and **B**. The B(1)-Se(1) distance [2.166(5) and 2.168(5) Å for the two independent molecules present in the unit cell] is comparable to the unique similar adduct reported in the literature.<sup>[27]</sup> The C(1)-Se(1)-B(1) angle [110.31(18) and 112.13(18) °] is close to a tetrahedral angle. The C(1)-Se(1) distance [1.863(4) and 1.855(4) Å] is significantly shorter than a pure C-Se single bond.<sup>[54]</sup> The C(1)-N(1) interaction [1.310(5) and 1.311(5) Å] possesses a considerable double bond character and both C(1) and N(1) displays an almost perfect sp<sup>2</sup> hybridization [sum angles at C(1) 360.0(6) and 359.9(6)°; sums angles at N(1) 359.5(6) and 359.8(6) °]. Such values are intermediate between those for a typical, isolated selenoamide (Se-C = 183.1 and C-N bonds = 132.1 pm, <sup>[55]</sup>) and a selenoiminium species (188.5 and 128.1 pm, respectively).<sup>[29,56]</sup> Finally, a weak  $\pi$ - $\pi$  interaction is present between the Ph ring bonded to C(1) and one C<sub>6</sub>F<sub>5</sub> ring bonded to B(1) [distances between the centroids 3.609 and 3.594 Å].<sup>[57]</sup>

In solution, the two methyl groups do not show any exchange peak at room temperature, indication that  $\Delta H_r^\ddagger$  is much higher than in the cases of **1** and **1-I**. The exchange process becomes visible at higher temperature values (343-373 K), allowing the measurement of  $\Delta H_r^\ddagger$  (23.6 kcal/mol  $\pm$  0.5). <sup>77</sup>Se NMR  $\delta$  for **1-B** is 578.5 ppm, i.e. much lower than those of **1-I** (776.7 ppm) and **1** (802.4 ppm) but higher than that of **2** (459.0 ppm)

Therefore, from these experimental results we can conclude that all the Lewis acids provide the same qualitative effect on the electronic structure of **1**, favouring the zwitterionic resonance structure, in which the C-N bond is double and the selenium hosts a formal negative charge, which

is partially donated to the LA. On the other hand, if the LA is too strong, EXSY NMR is not able to provide the rotational barrier value.

**3.2 Computational studies.** To investigate these findings in more detail, we performed various DFT analyses. The details of all the employed calculations are given in ESI.

Exploring the potential energy surface (PES) of the **1-I** adduct, several stable conformers can be found. In the most stable adduct (**1-I**<sup>1</sup>), iodine interacts with both the selenium ( $d_{\text{Se-I}} = 3.298 \text{ \AA}$ ) and aromatic ring of the phenyl group (see Figure 4). To assess the effect of these interactions separately, we also considered a conformer (**1-I**<sup>2</sup>) that contains only XB bond of selenium and iodine ( $d_{\text{Se-I}} = 3.375 \text{ \AA}$ ), and that (**1-I**<sup>3</sup>) contains mainly the interaction of iodine with the phenyl group. The iodine and the selenoamido moiety lie on the same plane in **1-I**<sup>1</sup> while they are perpendicular in **1-I**<sup>2</sup>.

The computed solution formation enthalpy of the most stable **1-I**<sup>1</sup> conformer is -8.00 kcal/mol. At the B3LYP-D3 level, the computed C-Se bond of **1-I**<sup>1</sup> (1.835  $\text{\AA}$ ) is longer than that of the isolated **1** (1.824  $\text{\AA}$ ). On the other hand, the C-N bond becomes shorter upon the formation of the adduct (1.340  $\text{\AA}$  in **1**; 1.331  $\text{\AA}$  in **1-I**<sup>1</sup>). Coherently, the computed rotational barrier is higher for **1-I**<sup>1</sup> (23.3 kcal/mol, respectively) than for **1** (16.9 kcal/mol). Considering a solution containing both **1-I**<sup>1</sup> (2.1 mM, see Table 2) and **1** (1.1 mM) the average value weighted on the concentrations, is 21.0 kcal/mol, in good agreement with the experimental values.

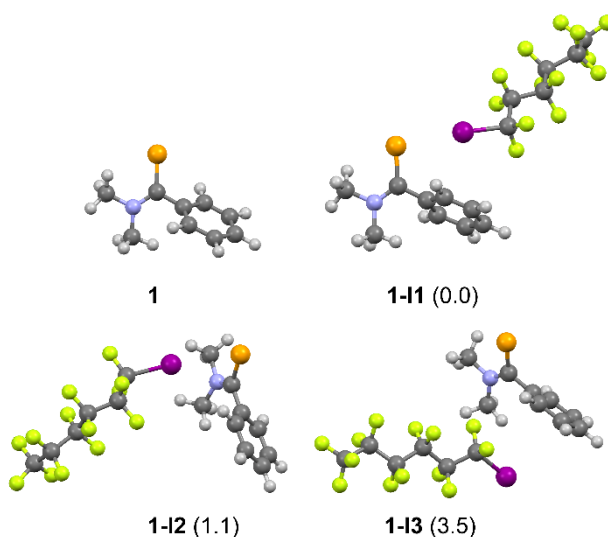


**Figure 4.** DFT-optimized geometries of three different conformers of **1-I**. The relative formation enthalpies in solution are reported in parenthesis(kcal/mol).

Interestingly, the C-Se distance passes from 1.825 to 1.801 Å for **1** and **TS(1)**, respectively (Table 4). This happens because, during the rotation of the C-NMe<sub>2</sub> bond, the latter is essentially single (1.431 Å), therefore no resonance is anymore possible and C-Se is double. In the presence of **I**, the situation is similar and C-Se passes from 1.835 to 1.809 Å for **1-I<sup>1</sup>** and **TS(1-I<sup>1</sup>)**, C-N from 1.332 to 1.425 Å and Se-I from 3.298 to 3.385 Å. Indeed, in **1-I<sup>1</sup>** the selenoamide is polarized and the selenium is able to establish a strong XB with the iodine. The rotation weakens the XB because it almost cancels out the polarization.

**Table 4.** Geometrical parameters (in Å) and relative enthalpies (in kcal/mol) for optimized structures.

Compound	C-Se	C-N	Se-X	$\Delta H^a$
<b>1</b>	1.825	1.339	-	0.0
<b>TS(1)</b>	1.801	1.431	-	16.9
<b>1-I<sup>1</sup></b>	1.835	1.332	3.298	-8.0
<b>TS(1-I<sup>1</sup>)</b>	1.809	1.425	3.356	15.4
<b>1-ICF<sub>3</sub></b>	1.838	1.333	3.388	-8.8
<b>TS(1-ICF<sub>3</sub>)</b>	1.807	1.425	3.385	9.9
<b>1-B</b>	1.858	1.323	2.471	-15.3
<b>TS(1-B)</b>	1.805	1.426	3.428	12.9
<b>1-BCl<sub>3</sub></b>	1.858	1.328	2.205	-9.3
<b>TS(1-BCl<sub>3</sub>)</b>	1.803	1.429	3.346	13.1
<b>1-Me<sup>+</sup></b>	1.892	1.309	1.964	-43.4
<b>TS(1-Me<sup>+</sup>)</b>	1.870	1.397	1.967	-10.4

<sup>a</sup>In the case of adducts, the energy with respect to the isolated fragments is reported.

The PESs of **1-Me<sup>+</sup>** and **1-B** are simpler, as the interactions are stronger, more directional and do not allow the presence of many conformers with similar energies. The stronger interactions have more marked effects on the geometries of **1**, lengthening the C-Se bond to up to 1.892 (**1-Me<sup>+</sup>**) and 1.858

*This item was downloaded from IRIS Università di Bologna (<https://cris.unibo.it/>)*

**When citing, please refer to the published version.**



Å (**1-B**). Conversely, the C-N bond shortens to 1.309 and 1.323 Å, respectively. These changes are nicely reflected in the computed  $\Delta H_r^\ddagger$  values, that are 33.0 and 28.2 kcal/mol. Also in this case the optimized geometries of TSs show a shorter C-Se bond and a longer Se-X (X = C or B) bond.

The high value of **1-Me**<sup>+</sup> is out of reach for the VT-EXSY NMR technique, mainly because of the boiling point of the solvent which creates an insurmountable upper limit for temperature. About **1-B**, the experimental value is quite lower (23.6 kcal/mol), but B(C<sub>6</sub>F<sub>5</sub>)<sub>3</sub> is known to give frustrated Lewis pairs (FLPs),<sup>[58]</sup> and also this Se-B bond is likely to become labile at high temperature. Under this assumption, the experimental value of  $\Delta H_r^\ddagger$  would be the concentration-weighted average value between the barrier in the adduct and in the free selenoamide. Being the latter much lower than the former, a small amount of free **1** would be enough to sensibly lower the average value.

Anyway, the interactions in the adducts deserve a more detailed characterization. For practical reasons, the large adducts **1-I1** and **1-B** will be reduced to **1-ICF<sub>3</sub>** and **1-BCl<sub>3</sub>**. The substitution has not a deep impact, as both the bond lengths and the values of  $\Delta H_r^\ddagger$  are very similar (see Table 4). The only relevant difference is between **1-B** and **1-BCl<sub>3</sub>**, as for the latter the  $\pi$ - $\pi$  dispersive interaction between the borane and the phenyl of **1** is obviously absent.

For **1**, the Natural Bond Orbital (NBO) analysis reveals that the sum of all the resonance structures (threshold 2%) with a single C-Se bond is 18.5% (*wgh1*), whereas the sum of those having a double C-Se bond have a relative weight of 33.3% (*wgh2*). The Natural Population Analysis (NPA) atomic charge for selenium is -0.15 and the natural bond orders are 1.64 and 1.30 for C-Se and C-N, respectively. Table 5 reports a comparison between the NBO results of **1** and its various adducts. As expected, the natural bond order of C-Se decreases as the new bond (Se-X, with X = I, B or C depending on the adduct) increases. The relative weights of resonance structures having C-Se or C=Se change accordingly, with the latter becoming less important as the LA strength increases.

**Table 5.** NBO analysis for **1**, **1-ICF<sub>3</sub>**, **1-BCl<sub>3</sub>** and **1-Me**<sup>+</sup>. Atomic charges are expressed in electrons, energy contribution (interaction energy  $E_{int}$ , charge transfer  $CT$ , electrostatic contributions  $El$  and repulsive forces  $Core$ ) are in kcal/mol.

System	$q(\text{Se})$	C-Se b.o.	Se-X b.o.	<i>wgh1</i>	<i>wgh2</i>	$E_{int}$	$CT$	$El$	$Core$
<b>1</b>	-0.15	1.64	-	18.54%	33.27%	-	-	-	-
<b>1-ICF<sub>3</sub></b>	-0.13	1.50	0.17 (X = I)	20.42%	17.44%	-2.7	-22.3	-18.2	37.8
<b>1-BCl<sub>3</sub></b>	0.25	1.30	0.85 (X = B)	19.35%	20.34%	-25.2	-195.9	-60.4	231.1

This item was downloaded from IRIS Università di Bologna (<https://cris.unibo.it/>)

**When citing, please refer to the published version.**

1-Me <sup>+</sup>	0.48	1.28	1.01 (X = C)	26.67%	18.64%	-157.7	-394.0	-93.7	330.0
-------------------	------	------	--------------	--------	--------	--------	--------	-------	-------

---

The Se-X interactions can be characterized by the natural energy decomposition analysis (NEDA). The interaction energy  $E_{int}$  between **1** and the second fragment (ICF<sub>3</sub>, BCl<sub>3</sub> or Me<sup>+</sup>) increases with the strength of the LA, but its composition varies with the nature of the latter. Indeed, for XB the charge transfer,  $CT$ , and electrostatic interactions,  $El$ , are quite similar, whereas for the selenium-borane and, to a larger degree, selenium-methyl interactions,  $CT$  is by far the most important contribution. This is due to the larger covalency of the strong contribution, but it is important to underline that also for XB  $CT$  is not negligible, being slightly larger than  $El$ .

Increasing the distance between the selenium and the methyl, all the NEDA components decay, but with different rates. In particular,  $El$  is the slowest one (see ESI), as expected, but even at the largest Se-Me<sup>+</sup> distance studied (3.964 Å),  $CT$  is still larger than  $El$  (-61.95 and -21.86 kcal/mol, respectively).

The second order perturbative analysis of the Fock matrix,  $E^{(2)}$ , evidenced the following orbital donor → acceptor interactions: for **1-ICF<sub>3</sub>**, a donation from the lone pair of selenium to the I-C antibonding orbital of ICF<sub>3</sub> (4.1 kcal/mol) and the C-N antibonding orbital (10.6 kcal/mol), for **1-BCl<sub>3</sub>** to the B-Cl antibonding orbitals (4.0 kcal/mol) and the C-N antibonding orbital (65.2 kcal/mol), for **1-Me<sup>+</sup>** to the C-H antibonding orbitals of the methyl (3.0 kcal/mol) and the C-N antibonding orbital (43.6 kcal/mol). Therefore, selenium allows the LA and the C-N bond to be indirectly electronically connected.

Similar conclusions can be drawn by the Extended Transition State-Natural Orbital for Chemical Valence (ETS-NOCV) analysis, that decomposes further the orbital contribution ( $E_{oi}$ ). In particular, for each adduct only one component ( $\Delta\rho_1$ , see Figure 5 and ESI) is relevant, all the others showing only polarization regions. In each adduct, a depletion region is around selenium, with a shape that resembles its  $p$  lone pair. Additional depletion regions are at the nitrogen, with the shape of its full  $p$  orbital perfectly fitting with our hypothesis: when the LA interacts with a lone pair of the selenium, electron density goes from the lone pair of the nitrogen to the  $\pi$  orbital between carbon and nitrogen, and at the same time the  $\pi$  orbital of the C-Se bond is depleted (the bond order decreases). The electron density donated by selenium accumulates between the latter and the LA, which results strongly polarized.

This item was downloaded from IRIS Università di Bologna (<https://cris.unibo.it/>)

**When citing, please refer to the published version.**

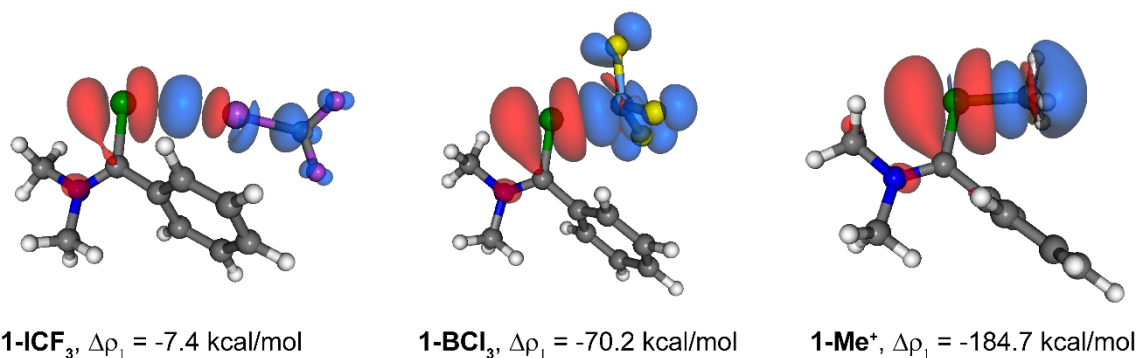


**Figure 5.** Isodensity surfaces (2 me a.u.<sup>-3</sup>) for the deformation maps relative to the NOCV  $\Delta\rho_1$  contribution of three adducts. The charge flux is red  $\rightarrow$  blue.

According to this analysis, the amount of charge ( $CT_1$ ) passing from the selenium to the LA is -90, -460 and -725 me (the negative sign solely depends on the direction of the flux and the choice of the molecule orientation), for **1-ICF<sub>3</sub>**, **1-BCl<sub>3</sub>** and **1-Me<sup>+</sup>**, respectively. To our delight,  $CT_1$  linearly correlates with  $\Delta H_r^\ddagger$  ( $r^2 = 0.910$ , Figure 6), demonstrating the potential of this strategy to characterize chemical interactions. Obviously, four points for such a wide span are not conclusive for a linear correlation, but they are a good starting point for more systematic investigations.

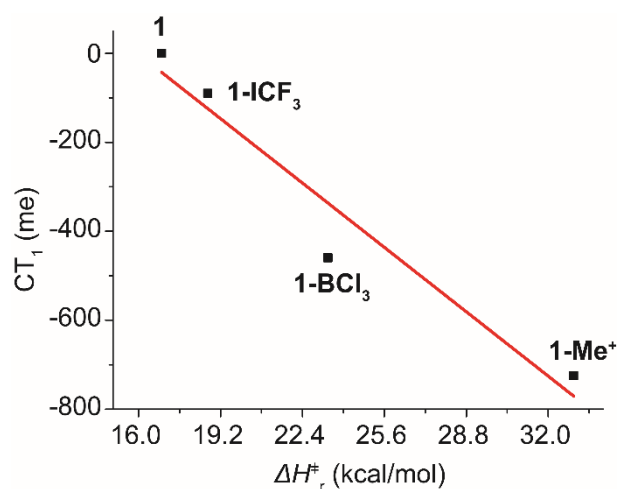


**Figure 6.** Linear correlation between the charge transfer  $CT_1$  and the rotational barrier of the C-N bond ( $\Delta H_r^\ddagger$ ).

#### 4. CONCLUSIONS

The adducts between the selenoamide **1** and various Lewis acids have been studied by NMR, specifically by  $^1\text{H}$  VT-EXSY, in order to use the electronic structure of **1** as a probe for the different interactions involved: halogen bonding in the case of fluorinated iodide compounds, dative bonds in the case of borane and purely covalent bond with the methyl cation. About the latter, an interesting acceleration of the reaction between methyl iodide and **1** has been noted in the presence of  $\text{IC}_6\text{F}_{13}$  and this phenomenon will be studied in detail.

The EXSY technique demonstrated to be useful in the quantification of the C-NMe<sub>2</sub> rotational barrier in the presence and absence of  $\text{IC}_6\text{F}_{13}$  and borane, but failed in the presence of stronger LAs, as methyl, because of the technical limits of the strategy, as the boiling point of the solvent. For the selenium-boron and selenium-methyl adducts, X-ray crystallography is a suitable technique to study the shortening of the C-Se bond, but the selenium-iodine adduct did not give X-ray quality crystals. Therefore, using a single experimental strategy for probing all the interactions remains challenging. Anyway, computational results well fit with experimental ones and have less limitations for the calculations of the rotational barriers, allowing to characterize in detail all the different adducts. Interestingly, a linear correlation seems to exist between the C-NMe<sub>2</sub> rotational barrier and the amount of charge donated by the selenium to the LA. More in depth and systematic studies are needed to confirm such a correlation.

Furthermore, the selenium probe could be improved to avoid the limitations here described, for example looking for a selenoamide with lower rotational barrier.

## 5. Electronic Supporting Information.

ESI contains supplementary tables, figures, NMR spectra, computational details and XYZ coordinates of optimized geometries. CCDC reference number 2159996 (**1-B**) contains the supplementary crystallographic data for the X-ray studies reported in this paper. These data can be obtained free of charge at [www.ccdc.cam.ac.uk/conts/retrieving.html](http://www.ccdc.cam.ac.uk/conts/retrieving.html) (or from the Cambridge Crystallographic Data Centre, 12, Union Road, Cambridge CB2 1EZ, UK; fax: (internat.) +44-1223/336-033; e-mail: [deposit@ccdc.cam.ac.uk](mailto:deposit@ccdc.cam.ac.uk)).

## 6. CONFLICTS OF INTEREST

There are no conflicts to declare.

*This item was downloaded from IRIS Università di Bologna (<https://cris.unibo.it/>)*

***When citing, please refer to the published version.***

## 7. ACKNOWLEDGEMENTS

University of Pisa is acknowledged for financial support (Fondi di Ateneo 2020). GC thanks Dr. Giovanni Bistoni and Dr. Altun Ahmet for helpful discussions.

## 8. REFERENCES

- [1] G. R. Desiraju, P. S. Ho, L. Kloo, A. C. Legon, R. Marquardt, P. Metrangolo, P. Politzer, G. Resnati, K. Rissanen, *Pure Appl. Chem.***2013**, 85, 1711–1713.
- [2] G. Cavallo, P. Metrangolo, R. Milani, T. Pilati, A. Priimagi, G. Resnati, G. Terraneo, *Chem. Rev.***2016**, 116, 2478–2601.
- [3] M. L. Liriano, J. Carrasco, E. A. Lewis, C. J. Murphy, T. J. Lawton, M. D. Marcinkowski, A. J. Therrien, A. Michaelides, E. C. H. Sykes, *J. Chem. Phys.***2016**, 144, 094703.
- [4] T. Brinck, A. N. Borrfors, *J. Mol. Model.***2019**, 25, 125.
- [5] C. C. Robertson, R. N. Perutz, L. Brammer, C. A. Hunter, *Chem. Sci.***2014**, 5, 4179–4183.
- [6] L. Zhao, M. von Hopffgarten, D. M. Andrada, G. Frenking, *Wiley Interdiscip. Rev. Comput. Mol. Sci.***2018**, 8, e1345.
- [7] T. Ziegler, A. Rauk, *Inorg. Chem.***1979**, 18, 1558–1565.
- [8] C. Wang, D. Danovich, Y. Mo, S. Shaik, *J. Chem. Theory Comput.***2014**, 10, 3726–3737.
- [9] C. Weinberger, R. Hines, M. Zeller, S. V. Rosokha, *Chem. Commun.***2018**, 54, 8060–8063.
- [10] A. C. C. Carlsson, A. X. Veiga, M. Erdélyi, *Top. Curr. Chem.***2015**, 359, 49–76.
- [11] M. Erdélyi, *Chem. Soc. Rev.***2012**, 41, 3547–3557.
- [12] P. L. Wash, S. Ma, U. Obst, J. Rebek, *J. Am. Chem. Soc.***1999**, 121, 7973–7974.
- [13] W. Herrebout, *Top. Curr. Chem.***2014**, 358, 79–154.
- [14] J. F. Bertrán, M. Rodríguez, *Org. Magn. Reson.***1979**, 12, 92–94.
- [15] M. T. Messina, P. Metrangolo, W. Panzeri, E. Ragg, G. Resnati, *Tetrahedron Lett.***1998**, 39, 9069–9072.
- [16] S. J. Pike, C. A. Hunter, L. Brammer, R. N. Perutz, *Chem. - A Eur. J.***2019**, 25, 9237–9241.
- [17] S. B. Hakkert, J. Gräfenstein, M. Erdelyi, *Faraday Discuss.***2017**, 203, 333–346.
- [18] G. Ciancaleoni, R. Bertani, L. Rocchigiani, P. Sgarbossa, C. Zuccaccia, A. Macchioni, *Chem. - A Eur. J.***2015**, 21, 440–447.
- [19] G. Ciancaleoni, *Magnetochemistry***2017**, 3, 30.

This item was downloaded from IRIS Università di Bologna (<https://cris.unibo.it/>)

**When citing, please refer to the published version.**

- [20] C. J. Serpell, N. L. Kilah, P. J. Costa, V. Félix, P. D. Beer, *Angew. Chemie - Int. Ed.***2010**, *49*, 5322–5326.
- [21] G. Ciancaleoni, A. Macchioni, L. Rocchigiani, C. Zuccaccia, *RSC Adv.***2016**, *6*, 80604–80612.
- [22] A. C. C. Carlsson, J. Gräfenstein, A. Budnjo, J. L. Laurila, J. Bergquist, A. Karim, R. Kleinmaier, U. Brath, M. Erdélyi, *J. Am. Chem. Soc.***2012**, *134*, 5706–5715.
- [23] S. A. Difranco, N. A. MacIulis, R. J. Staples, R. J. Batrice, A. L. Odom, *Inorg. Chem.***2012**, *51*, 1187–1200.
- [24] B. S. Billow, T. J. McDaniel, A. L. Odom, *Nat. Chem.***2017**, *9*, 837–842.
- [25] G. Ciancaleoni, L. Biasiolo, G. Bistoni, A. Macchioni, F. Tarantelli, D. Zuccaccia, L. Belpassi, *Chem. - A Eur. J.***2015**, *21*, 2467–2473.
- [26] H. D. Arman, E. R. Rafferty, C. A. Bayse, W. T. Pennington, *Cryst. Growth Des.***2012**, *12*, 4315–4323.
- [27] D. Holschumacher, C. G. Daniliuc, P. G. Jones, M. Tamm, *Z. Naturforsch B***2011**, *66*, 371–377.
- [28] G. Ciancaleoni, *Proc. 1st Int. Electron. Conf. Catal. Sci. Novemb. 2020, MDPI Basel, Switz.***2021**, 7538.
- [29] Y. Mutoh, T. Murai, *Org. Lett.***2003**, *5*, 1361–1364.
- [30] K. A. Jensen, J. Sandström, *Acta Chem. Scand.***1969**, *23*, 1911–1915.
- [31] G. Marrazzini, C. Gabbiani, G. Ciancaleoni, *ACS Omega***2019**, *4*, 1344–1353.
- [32] G. M. Li, J. H. Reibenspies, R. A. Zingaro, *Heteroat. Chem.***1998**, *9*, 57–64.
- [33] J. S. Hartman, G. J. Schrobilgen, P. Stilbs, *Can. J. Chem.***1976**, *54*, 1121–1129.
- [34] D. Bibelayi, A. S. Lundemba, F. H. Allen, P. T. A. Galek, J. Pradon, A. M. Reilly, C. R. Groom, Z. G. Yav, *Acta Crystallogr. Sect. B Struct. Sci. Cryst. Eng. Mater.***2016**, *72*, 317–325.
- [35] G. Ciancaleoni, *Phys. Chem. Chem. Phys.***2018**, *20*, 8506–8514.
- [36] F. S. S. Schneider, G. F. Caramori, R. L. T. Parreira, V. Lippolis, M. Arca, G. Ciancaleoni, *Eur. J. Inorg. Chem.***2018**, *2018*, 1007–1015.
- [37] R. Montis, M. Arca, M. C. Aragoni, A. Bauzá, F. Demartin, A. Frontera, F. Isaia, V. Lippolis, N. Bricklebank, M. Schröder, C. Wilson, G. Verani, *CrystEngComm***2017**, *19*, 4401–4412.

This item was downloaded from IRIS Università di Bologna (<https://cris.unibo.it/>)

**When citing, please refer to the published version.**

- [38] J. Viger-Gravel, J. E. Meyer, I. Korobkov, D. L. Bryce, *CrystEngComm***2014**, *16*, 7285–7297.
- [39] P. Bhattacharyya, J. D. Woollins, *Tetrahedron Lett.***2001**, *42*, 5949–5951.
- [40] G. M. Sheldrick, *SADABS-2008/1 - Bruker AXS Area Detector Scaling and Absorption Correction*, Madison, Wisconsin, USA, **2008**.
- [41] G. M. Sheldrick, *Acta Crystallogr. Sect. C Struct. Chem.***2015**, *71*, 3–8.
- [42] A. L. Spek, *PLATON-a Multipurpose Crystallographic Tool*, Utrecht, The Netherlands, **2005**.
- [43] N. M. Alexej Jerschow, *J. Magn. Reson.***1997**, *375*, 372–375.
- [44] R. Mills, *J. Phys. Chem.***1973**, *77*, 685–688.
- [45] A. Macchioni, G. Ciancaleoni, C. Zuccaccia, D. Zuccaccia, *Chem. Soc. Rev.***2008**, *37*, 479–489.
- [46] F. Neese, *Wiley Interdiscip. Rev. Comput. Mol. Sci.***2017**, *8*, e1327.
- [47] S. Grimme, S. Ehrlich, L. Goerigk, *J. Comput. Chem.***2011**, *32*, 1456–1465.
- [48] S. Grimme, J. Antony, S. Ehrlich, H. Krieg, *J. Chem. Phys.***2010**, *132*, 154104.
- [49] E. D. Glendening, J. K. Badenhoop, A. E. Reed, J. E. Carpenter, J. A. Bohmann, C. M. Morales, C. R. Landis, F. Weinhold, *NBO 6 (Theoretical Chemistry Institute, University of Wisconsin, Madison, WI, 2013)*; [Http://Nbo6.Chem.Wisc.Edu/](http://Nbo6.Chem.Wisc.Edu/), **n.d.**
- [50] E. D. Glendening, C. R. Landis, F. Weinhold, *Wiley Interdiscip. Rev. Comput. Mol. Sci.***2012**, *2*, 1–42.
- [51] M. Radoń, *Theor. Chem. Acc.***2008**, *120*, 337–339.
- [52] A. Sørensen, B. Rasmussen, M. Pittelkow, *J. Org. Chem.***2015**, *80*, 3852–3857.
- [53] T. Wirth, *Organoselenium Chemistry: Synthesis and Reactions*, Wiley-VCH Verlag GmbH & Co. KGaA, Weinheim, Germany, **2011**.
- [54] L. Busetto, F. Marchetti, S. Zacchini, V. Zanotti, *Organometallics***2006**, *25*, 4808–4816.
- [55] G. M. Li, J. H. Reibenspies, A. Derecskei-Kovacs, R. A. Zingaro, *Polyhedron***1999**, *18*, 3391–3399.
- [56] The typical length for a single Se-C bond is 196 pm.
- [57] H. W. Roesky, M. Andruh, *Coord. Chem. Rev.***2003**, *236*, 91–119.
- [58] D. W. Stephan, G. Erker, *Angew. Chemie - Int. Ed.***2015**, *54*, 6400–6441.

This item was downloaded from IRIS Università di Bologna (<https://cris.unibo.it/>)

**When citing, please refer to the published version.**

*This item was downloaded from IRIS Università di Bologna (<https://cris.unibo.it/>)*

***When citing, please refer to the published version.***